



A GEANT-based package for determination of the *Pamir* experiment X-ray emulsion chamber response

A.S. BORISOV^a, V.G. DENISOVA^a, V.I. GALKIN^b, M.G. KOGAN^a, E.A. KANEVSKAYA^a, K.A. KOTELNIKOV^a, R.A. MUKHAMEDSHIN^{c*}, S.I. NAZAROV^a, V.S. PUCHKOV^a

(a) *Lebedev Physical Institute, Moscow, 119991 Russia*

(b) *Skobel'tsyn Institute of Nuclear Physics, Moscow, 119992 Russia*

(c) *Institute for Nuclear Research, Moscow, 117312 Russia*

*muhamed@sci.lebedev.ru

Abstract: The *ECSim* 2.0 package version is released aimed at simulation of the development of nuclear-electromagnetic cascades initiated by different particles in stratified media with a particular attention paid to a response of X-ray emulsion chambers. Features of *ECSim* 2.0 and results of simulation are discussed for the case of the passage of electrons and γ -rays through the Γ -block of *Pamir* experiment's X-ray emulsion chambers.

Introduction

The *ECSim* 2.0 package version is intended for detailed 3D-simulation of development of nuclear-electromagnetic cascades (NEC) initiated by different particles, from protons to nuclei, in X-ray emulsion chambers (XREC) on the basis of GEANT 3.21 package. It is based on the *ECSim* 1.0 [1] used by RUNJOB experiment which, however, cannot be directly applied to the simulation of the ground-based experiments detecting secondary particles (π , K etc.). The *ECSim* 2.0 code can be used in a broader field of problems for simulations of NECs in complex and multi-layer media in a wide range of energies from 10 keV to ~ 100 PeV, accounting for specific measuring procedures exploited in XREC experiments. This paper is devoted to the simulation of the *Pamir* experiment XREC response.

Simulation of particle propagation processes through XREC

The *ECSim* v. 2.0 package incorporates:

- the LPM effect for electromagnetic processes (following version 1.0);
- generation of hadron-hadron and hadron-nucleus

interactions at $E > 80$ GeV using the QGSJET model [2] (following version 1.0);

- simulation of NECs initiated in the chamber by hadrons of various types (p/\bar{p} , n/\bar{n} , π , K/\bar{K} and so on), e^\pm , γ -rays at different incident angles (new feature);
- tracking of correlated groups of particles (γ , e^\pm , h) of high energy ($E \gtrsim 4$ TeV), the so-called γ - h families, passing through XREC that requires substantial changes in the logic of processing of these events (new feature);
- simulation of the passage of superhigh-energy muons with cross sections for bremsstrahlung, e^+e^- pair production, knock-on electron production and nuclear interaction similar to those used in GEANT4 (new feature);
- for lead as the most frequently used high-Z absorber the pair production cross section was corrected for LPM effect, i.e., the muon cross section was reduced by a factor proportional to the γ -ray cross section decrease at the same energy (new feature);
- LPM-corrected cross sections for bremsstrahlung by electrons and pair production by γ -rays were extended up to 10^{19} eV (new feature).

ECSim 2.0 makes it possible to analyze the NEC development in any stratified medium. Test results show good agreement with other authors' data. For

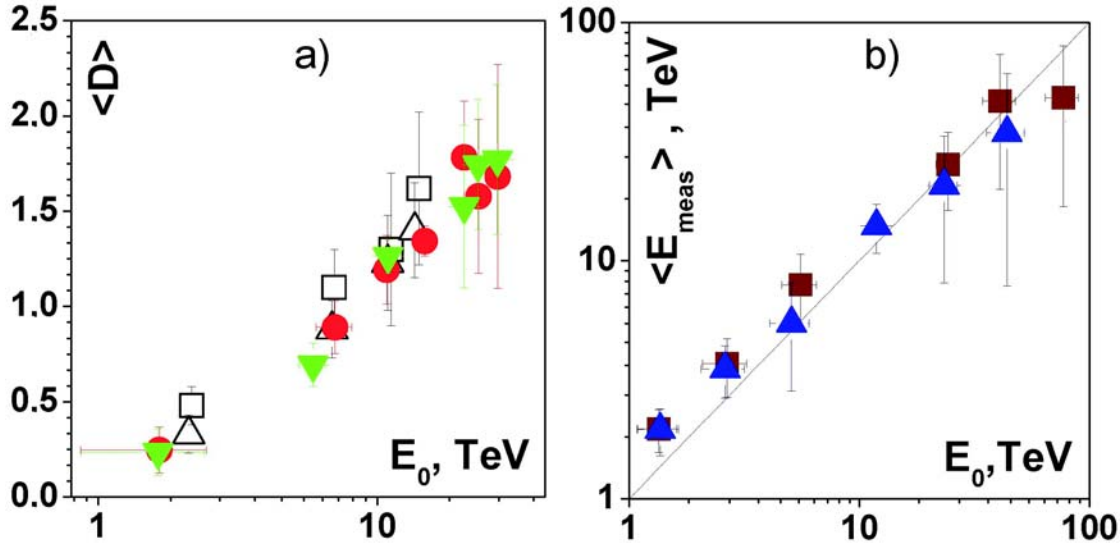


Figure 1: (a) Average optical density $\langle D \rangle$ dependence on primary energy $\langle E_0 \rangle$ at 9-r.l. depth for γ -rays (circles) and electrons (triangles), incident angles are $15^\circ \leq \theta \leq 25^\circ$. Empty squares and triangles are the data of [4] for e/γ flux with incident angles $0^\circ \leq \theta \leq 5^\circ$ and $15^\circ \leq \theta \leq 25^\circ$, respectively, at 9-r.l. depth. (b) Average "measured" energy $\langle E_{\text{meas}} \rangle$ dependence on primary energy E_0 of electrons (squares) and γ -rays (triangles) at 9-r.l. depth, incident angles are $0^\circ \leq \theta < 12^\circ$. Straight line is the case $\langle E_{\text{meas}} \rangle = E_0$.

instance, the n_{ch} transition curves in Pb in cascades initiated by γ -rays of energy $E_0 = 1$ PeV and traced down to $E_{\text{min}} = 1$ TeV agree with results [3].

Simulation of dark spot formation

One of the most important points of XREC technique is the measurement of darkness of spots on X-ray film produced by electron-photon cascades (EPC) and reconstruction of EPC energies. To simulate the darkness measurement procedure, the field of view of the measuring diaphragm is divided into square cells of linear size l_{cell} . The *Pamir* experiment used measuring diaphragms with radii $R_d \simeq 48 - 140 \mu\text{m}$. A relation used by the *Pamir* experimenters for calculation of darkness density is $D = D_0\{1 - \exp(-s\rho)\}$. Here $s = 3.25 \pm 0.13 \mu\text{m}^2$, ρ is the number of particles per unit square.

While charged particles cross the emulsion plane, their number N_i in i th cell is summed up and recorded, and the darkness D_i is calculated with the use of the above-given relation. For all K cells

visible in the field of view of the measuring diaphragm of given shape and size, the total "measured" darkness D_{tot} is calculated as follows

$$D_{\text{tot}} = \lg K - \lg \sum_{i=1}^K 10^{-D_i(N_i)}.$$

Particularly, this approach enables to reproduce the former *Pamir* procedure for darkness measurement by a circle diaphragms of given radius R_d : D_{tot} value is calculated and then the standard *Pamir* procedure is used to evaluate the cascade energy on the basis of the measured darkness.

It is important to optimize the cut-off energy E_{min} for cascade secondary particle tracing. It was shown that the cut-off optimal value is $E_{\text{min}} = 1$ MeV. Lower values do not improve the simulation accuracy but do increase the simulation time.

What follows are simulations of the *Pamir* experiment XREC Γ -block which incorporates 5 cm (9 r.l.) of lead with two double-layer X-ray films beneath as well as calculations of darkening spots produced by cascades traversing the X-ray films.

The gap between the lead surface and downstream sensitive film layer was taken to be $500 \mu\text{m}$, and $l_{\text{cell}} = 16 \mu\text{m}$ was used for the cell size within diaphragm inner region while smaller l_{cell} values

were applied to the diaphragm near-to-boundary ring.

Single particles

The process of measurement of single particle spectra of electromagnetic particles (e^\pm, γ) was analyzed. It was assumed that they were distributed in energy according to a power-law differential spectrum of power index $\gamma = -3.0$. Their angular distribution was assumed to be of the form $dN/d\Omega \sim \cos^6 \theta$ within the zenith angle domain $0^\circ < \theta \leq 36^\circ$.

Fig. 1(a) shows simulation results for the average optical density $\langle D \rangle$ vs. primary energy E_0 at $R_d = 48 \mu\text{m}$ for electrons and γ -rays. One can see that these data agree well with the results [4] at $R_d = 50 \mu\text{m}$.

Figs. 1(b) and 2 present the data obtained while averaging over three diaphragm radii ($R_d = 48, 84,$ and $140 \mu\text{m}$).

Fig. 1(b) shows the average "measured" energy $\langle E_{\text{meas}} \rangle$ at 9-r.l. depth versus primary energy E_0 . It is clear that the standard *Pamir* procedure of energy reconstruction works well at $E_0 = 4-70 \text{ TeV}$. At $E_0 > 70 \text{ TeV}$ the procedure underestimates the "measured" energy for both γ -rays and electrons but the effect is more pronounced for γ -rays. This is due to the fact that the standard procedure does not take the LPM-effect into account properly. It was also shown that the standard procedure takes proper account of the gaps between the lead plates and films.

Fig. 2 shows "measured" energy spectra. The power-law indices are $\gamma_{\text{meas}}^e = -3.03 \pm 0.06$ for electrons and $\gamma_{\text{meas}}^\gamma = -3.12 \pm 0.04$ for γ -rays. Thus, the "measured" spectra are close to the incident spectra by the slopes but still are slightly steeper due to the above-mentioned incorrect accounting for the LPM effect.

Correlated groups of particles

While tracking groups of correlated particles (γ, e^\pm , hadrons or so-called γ - h families) through XRECs, one must substantially change the logic of their processing as the total darkness picture in a sensitive layer is produced by all the particles (by

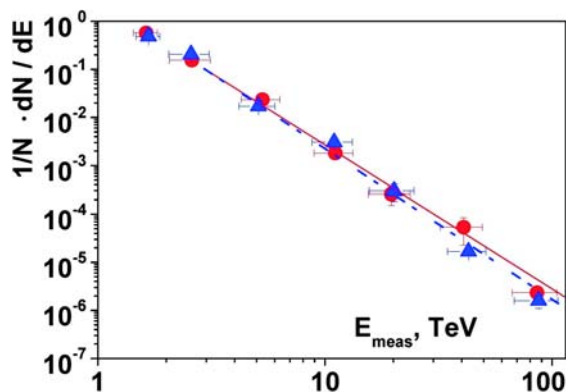


Figure 2: "Measured" energy spectra (averaged over three diaphragm-radius values) of electrons ($\bullet, —$) and γ -rays ($\Delta, - - -$).

EPCs, more precisely) of the family. Spots overlap frequently, especially at higher energies. In this case the following algorithm is applied:

- 1) The observation area is divided into cells of size l_{cell} ; number of charged particles produced in each cell by all EPCs initiated by family particles in XREC is calculated.
- 2) While using the simulation data on numbers of particles in cells produced by each of the EPCs (independently of other EPCs), the darkness "measured" by a diaphragm with radius R_d , centralized in relation to a cell with maximum numbers of particles, is calculated for each EPC.
- 3) A procedure of maximization of the "measured" darkness is applied, i.e., the diaphragm center walks around the maximum darkness cell over several (depending on presence of spots) neighboring cells; the "measured" darkness at each stage is calculated; the maximum darkness for the diaphragm applied is found.
- 4) For more exact energy determination, the so called "near-by" background is calculated, i.e., the background produced by all the family EPCs in the family area (sufficiently far from any EPC).
- 5) A procedure of spot visibility identification (or spot recognition) is applied taking into account two main effects of overlapping of neighboring spots produced by different EPCs.

These effects are as follows: 1) overestimation of "measured" energies; 2) spots produced by some EPCs are not visible against the total background or that produced by other EPCs. To avoid these

effects, which could lead to serious distortions of calculated results, the following procedure of spot visibility identification has been designed.

1) Let us consider a spot (named below spot 1) with darkness D_1 . If there is no other spots with darkness $D_i > D_1$ (by diaphragm $R_d = 48 \mu\text{m}$) at a distance of $\lesssim 1$ mm from the center of spot 1, then spot 1 is treated as visible. Otherwise the analysis is continued.

2) The Rayleigh's criterion is used to determine the degree of the spot visibility as follows. It is taken that the spot 1 is seen against the background produced by spot 2 with $D_2 > D_1$, if the maximum darkness of spot 1, D_{1max} , is higher than a minimum darkness D_{1-2min} ("measured" during the drift toward the center of spot 2) not less than by 30 percent. In doing so, the procedure searches for D_{1-2min} by deviating by some distance, which depends on size of spot 1, from the direct line connecting the centers of both the spots. Furthermore, the maximum distance restricting the searching area is equal to the minimum one from two values, i.e., either the half distance between the centers of both the spots or the half distance from the spot center to a place where the spot darkness is really not distinguished against the background. To calculate the spot visibility by the Rayleigh's criterion, diaphragms of different radii are used depending on spot size. The average darkness is also calculated along the line connecting the centers of both the spots over the above-defined distance. The spot 1 is treated as invisible, if this darkness "measured" by the same diaphragm appears to be higher than D_{1max} .

Conclusion

The *ECSim* 2.0 package is designed to simulate both the NEC development in complex-structure medium at $10 \text{ keV} \lesssim E_0 \lesssim 100 \text{ PeV}$ and γ - h family energy measurement procedure applied in XREC experiments.

It is shown that the *Pamir* standard procedure of energy determination by darkness values measured within circular apertures works well at $E_\gamma = 4-70$ TeV.

Acknowledgements

This work is supported by the RFBR, projects 05-02-17599, 05-02-16781, 06-02-16606, 06-02-16606, 06-02-16969; and Ministry of Education and Science, projects SS-5573.2006.2, 02.518.11.7084)

References

- [1] Galkin V.I., Nazarov S.N. Simulation of cosmic ray passage through an emulsion chamber *Preprint SINP MSU* 1999. 99-14/572
- [2] Kalmykov N.N. and Ostapchenko S.S. QGS model taking into account jets and EAS *Yad. Fiz.* 58 (1994) 21.
- [3] 02.518.11.7084 Okamoto M., Shibata T. *Nucl. Instrum. & Methods in Phys. Res. A*257 (1987) 155.
- [4] Haungs A. *Nucl. Phys. B* (Proc. Suppl.), 2006. V. 151. P. 215-222.